Optimization of a coupled launching process considering hydrodynamic interaction effects

IOP Conf. Series: Materials Science and Engineering 1288 (2023) 012021 doi:10.1088/1757-899X/1288/1/012021

Optimization of a coupled launching process considering hydrodynamic interaction effects

L Altenbach[1], M Wermbter[1], P Marleaux[1] and M Abdel-Maksoud[1]

[1] Institute for Fluid Dynamics and Ship Theory, Hamburg University of Technology (TUHH), Am Schwarzenberg-Campus 4, 21073 Hamburg, Germany

E-mail: lukas.altenbach@tuhh.de

Abstract. Crane-assisted launching and recovering of small boats from a large vessel is common in a wide range of operational scenarios and may be required during research missions or in emergency situations for rescue boats. As the mothership moves in natural irregular seas, the resulting accelerations and motions of the small boat can lead to dangerous situations, such as a collision between the mothership and the small boat or a slamming of the small boat onto the free water surface can occur, posing a great danger to the people involved. In the paper, the development of a coupled simulation method for the motions of the mothership and the small boat during the launching in the time-domain is described. The developed simulation method is based on the impulse response function. The implementation of the suspension on a crane is realised by a holonomic constraint and a Lagrange's equation. The parameter influencing the launching operation include the current sea state, the stationary wave field induced by the motherships forward speed, at which the small boat is launched and the initial position of the small boat relative to the water surface. By varying the above mentioned parameters, the process can be optimised for different sea states in terms of forces and accelerations. In considering the forward speed of the mother boat during the launching process, it can be observed that in many cases the small boat is operated at high Froude numbers of greater than 0.4. This leads to an exceedance of the operational limits of the programmes used in this paper.

1. Introduction

The aim of this paper is to analyse the behaviour of a small craft launched into the water by crane with forward speed from a mothership. Simplified, the launching procedure can be divided into three steps. First, the small craft is suspended freely from the crane without the influence of hydrodynamic forces. In the second step, the boat is lowered and comes into contact with the water surface. Finally, the boat moves independently without the influence of the crane cable next to the mother ship. When touching down on the water surface, the sudden hydrodynamic forces cause high accelerations. These might cause damage to persons and to the hull of the small craft. With regard to human factors for safe operation, limit values for transverse and vertical accelerations have been summarised, as Nordforsk criteria [1]. Many parameters can influence the transverse and vertical accelerations such as the distance between the two ships, the initial trim angle of the small boat, the lowering speed as well as the forward speed of the coupled system of mother ship and boat. Since launching operations with moderate forward motion of the mothership lead to high Froude numbers of the small boat. In this case, the optimal range of applicability of the method applied for the calculation of the ship motion based on the impulse response functions [2, 3], with coefficient calculation by the Rankine Panel Method [4],

is exceeded. For example, in such cases programs based on the 2D+t method and explicitly developed for the simulation of fast planing boats can provide reasonable results [5]. Due to the different hull geometries of dinghies, the focus in this paper is not to provide general predictions about the motion behaviour of the boat and the loads on the hull, but to analyse the influence of specific boundary conditions on the parameters mentioned above.

2. Mathematical model

2.1. Impulse response method IMPRES

The simulation program IMPRES [3] is a method for determining ship motions in the time domain. It uses the approach of Cummins [2] to calculate a motion response to a force from the decaying impulses of the past time steps. Due to the calculation with values from transfer functions and the assumption of harmonic motions, only linear motion responses can be realised. The equation of motion to be solved has the following notation:The equation of motion to be solved has the following notation:

$$(\mathbf{M}+\mathbf{A})\ddot{\boldsymbol{\xi}}(t)+\int_0^\infty \mathbf{B}(\tau)\dot{\boldsymbol{\xi}}(t-\tau)\,d\tau+\mathbf{S}\boldsymbol{\xi}(t)=\sum \mathbf{F}(t). \tag{1}$$

M is the inertia matrix, **A** is the hydrodynamic mass matrix, **S** is the restoring force matrix and **B** is the retardation function matrix, which includes the motion influence from previous time steps. **F** denotes the time-dependent excitation forces. To speed up the calculation, pre-calculated values for hydrodynamic mass and damping and transfer functions of the motion for different wave frequencies are provided in frequency domain. For this purpose, the method *pan*FDS is used, which is explained in 2.2 in more detail. These calculations are performed in the initialisation phase of the IMPRES simulation before the first time step. Subsequently, the acting forces are considered in the equation of motion from equation 1 and the system of equations is solved according to the accelerations in all six degrees of freedom. The motions of the hull can be determined by temporal integration. The generation of the irregular seaway results from the superimposition of individual linear wave components. A Jonswap wave spectrum is used as the distribution basis for the individual wave frequencies.

2.2. Threedimensional panel code panFDS

In order to make time-efficient predictions about motions and forces on ships, calculation methods in the frequency domain are often used. As mentioned above, IMPRES uses such pre-calculated values. These are calculated using the *pan*FDS method. With *pan*FDS, forces on and motions of symmetrical single hull ships in regular waves can be simulated. The fluid around the ship is assumed to be a potential flow. This implies a velocity potential from which pressures and hence forces can be calculated. When travelling with forward speed, a stationary wave system is developed, which moves along with the ship. This is not calculated by *pan*FDS, but read in as input from a Rankine Source method [4, 6]. Three-dimensional panels are used to discretise the hull and the water surface. As output, the program generates files with complex values for hydrodynamic mass and damping, diffraction or drift forces and transfer functions of motion responses to waves of different frequencies.

2.3. Wave interaction between the ships

The wave interaction is mainly caused by the stationary wave system of the mothership. This has an influence on the suspended small craft at higher speeds. At lower speeds, this influence decreases due to the lower wave height and can be considered to be negligible beyond a certain threshold. After launching, a stationary wave field also emanates from the small craft, the influence of which on the large ship can also be neglected. The stationary wave field is calculated

in the initialisation process by using the Rankine Panel Method. The wave potential is calculated from the associated source strengths, which are determined iteratively. Two grids are generated for the calculation of the transfer functions. One is the surface grid for the ship hull and the other is the grid for discretising the water surface. The deformation of the water surface is determined from the potential-based velocity and pressure field around the ship. In each iteration, the grids of water surface and body are adapted to the deformation of the free surface and the initial floating position is also adjusted to the prevailing pressure condition due to changes forces and moments. While the grid resolution of the hull grid remains the same, the grid resolution of the free surface changes according to the surface deformation. The shorter the wave length, the smaller the panel size of the free surface grid becomes [4]. This leads to a limitation of the method for both very high and very low forward velocities. For low velocities, the computational effort becomes large due to an increasing number of panels and for large velocities, details of the hull are insufficiently accurately represented due to coarse mesh. On this evidence, the different velocities used in the following have been selected. Figure 1 shows the stationary wave field of the KCS (Kriso Container Ship [7]) at a Froude number of $Fn = 0.211$ in still water conditions. The blue colour stands for a wave crest. Red defines a wave trough.

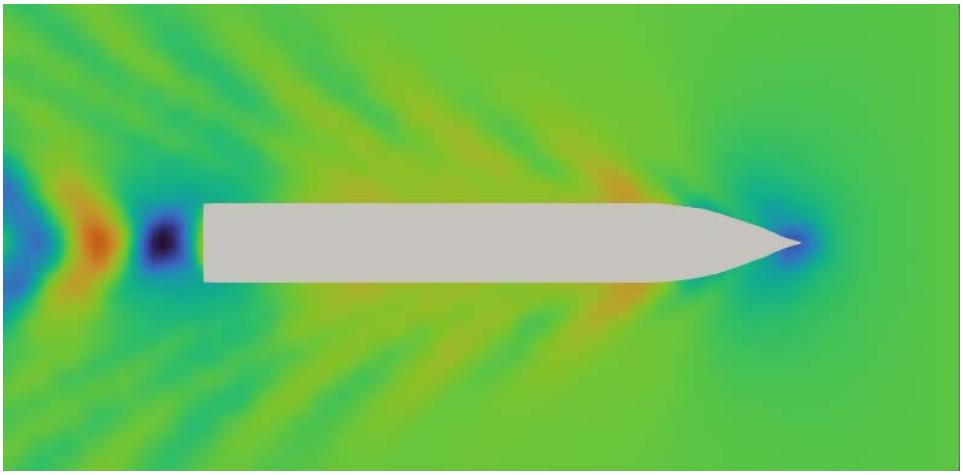

Figure 1. Stationary wave field of the KCS hull at $Fn = 0.211$.

2.4. Modelling of the crane suspension

During the launching process, the small craft is attached to the hook of a crane installed on the mothership. The motions of the mothership cause the tip of the crane and the dinghy suspended from it to move accordingly. By constantly extending the crane rope, the small craft is lowered from its initial position on the crane to the level of the water surface. Until the small craft generates sufficient buoyancy to float on its own, a constraining force acts on the small craft, which in the stationary state acts in the opposite direction to the weight force and is of equal magnitude. The suspension on a crane rope is solved by means of a holonomic constraint and a Lagrangian equation [8]. The holonomic constraint describes a property in the form of a function $\mathbf{g}$, which does not change over time. In general,

$$\mathbf{g}(\boldsymbol{\xi}, t) = 0 \tag{2}$$

is the form of the constraint. In the particular case of a rope suspension, the function $\mathbf{g}$ is defined by

$$\mathbf{g}(\boldsymbol{\xi}, t) = (\boldsymbol{\xi}_{1q} - \boldsymbol{\xi}_{1p})^2 + (\boldsymbol{\xi}_{2q} - \boldsymbol{\xi}_{2p})^2 + (\boldsymbol{\xi}_{3q} - \boldsymbol{\xi}_{3p})^2 - l^2 = 0. \tag{3}$$

Here, the indice p describes the end of the rope at the crane tip and the indice q defines the point on the small boat and l the rope length. With the definition for the vector $\mathbf{Q}$

$$\mathbf{Q} = \frac{\partial \mathbf{g}}{\partial \boldsymbol{\xi}} \tag{4}$$

the rope force F_z acting on the boat is given by

$$\mathbf{F}_z = \mathbf{Q}^T \boldsymbol{\lambda}. \tag{5}$$

$\boldsymbol{\lambda}$ is the Lagrangian coefficient resulting from the solution of the extended system of equations in 8. For the right-hand side of the equation system, the vector $\mathbf{G}$ is needed, which results from the second time derivative of equation 4. Since both temporal and spatial differentiation occur, the total derivative must be formed, which are given in equation 6 and 7.

$$\mathbf{Q}\dot{\boldsymbol{\xi}} = -\frac{\partial \mathbf{g}}{\partial t} \tag{6}$$

$$\mathbf{Q}\ddot{\boldsymbol{\xi}} = -\frac{\partial (\boldsymbol{Q}\dot{\boldsymbol{\xi}})}{\partial \boldsymbol{\xi}}\dot{\boldsymbol{\xi}} - 2\frac{\partial^2 \mathbf{g}}{\partial \boldsymbol{\xi} \partial t}\dot{\boldsymbol{\xi}} - \frac{\partial^2 \mathbf{g}}{\partial t^2} = \mathbf{G} \tag{7}$$

The original system of equations consisting of six equations for solving the motion is extended by one Lagrange equation for each constraint. In this case, a set of seven equations is created with one constraint.

$$\begin{bmatrix} \mathbf{M} + \mathbf{A} & \mathbf{Q}^T \\ \mathbf{Q} & \mathbf{0} \end{bmatrix} \begin{bmatrix} \ddot{\boldsymbol{\xi}} \\ -\boldsymbol{\lambda} \end{bmatrix} = \begin{bmatrix} \mathbf{F}_H + \mathbf{F}_A + \mathbf{A}\ddot{\boldsymbol{\xi}} - \mathbf{K} \\ \mathbf{G} \end{bmatrix} \tag{8}$$

3. Simulation

For the purpose of optimisation, different simulation setups are investigated and the results are compared. Some settings are kept the same for all simulations. The KCS hull is downscaled by a factor of 4 and used as the mothership and the planing boat's geometry is the prismatic hull shape by Brown and Klosinski [9]. The main dimensions of the two ships are listed in table 1. The initial scenario for the simulation is shown in figure 2.

Table 1. Main dimensions of mothership and small craft.

Parameter	Mothership	Small craft
L_{PP}	57.7 m	12.0 m
B	8.0 m	2.29 m
D	2.7 m	0.348 m

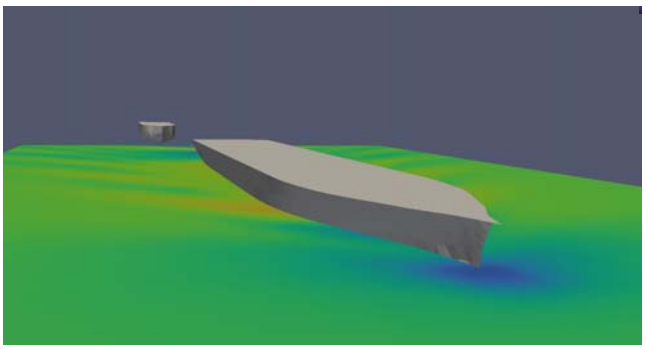

Figure 2. Illustration of the launching process before lowering with the small craft hanging from the crane.

Launching of the small boat from the initial suspended position starts five seconds after the begin of simulation. A wave spectrum is used for modelling the seaway. Two sea states with different zero upcrossing periods T_z are selected from the North Atlantic scatter table [10]. The significant wave height for both sea states is $H_s = 1.5\,\mathrm{m}$ and the periods are $T_{z1} = 7.5s$ and $T_{z2} = 8.5\,\mathrm{s}$, respectively. The seaway is modelled by a Jonswap spectrum and is consists of 30 wave components. For comparability, the phase angles, periods and heights of the individual waves are identical for all simulations. The wave direction is opposite to the ship's direction of travel. The wavelength of the ship's own wave system is approximated by $\lambda_{\mathrm{ship}} = 2\pi\, L_{\mathrm{ship}}\, Fn^2$ and therefore increases quadratically with the speed. The refinement of the free surface grid, which is used in *pan*FDS to calculate the stationary wave field, is proportional to the wavelength. This results in a strongly increased computational effort when the grid of the Rankine source method becomes finer due to the shorter wave. All six degrees of freedom are enabled for the mothership and small craft. The mothership's motions are transmitted to the boat via the suspension system.

Table 2. Froude numbers for different ships and forward speeds.

Parameter	Mothership	Small craft
Fn ($v = 3\frac{\mathrm{m}}{\mathrm{s}}$)	0.126	0.277
Fn ($v = 4\frac{\mathrm{m}}{\mathrm{s}}$)	0.168	0.369
Fn ($v = 5\frac{\mathrm{m}}{\mathrm{s}}$)	0.211	0.461

The lateral gap between the mothership and small boat (1.0 B, 2.0 B and 3.0 B) is considered as the parameter to be varied. B stands for the width of the small craft. Furthermore, the initial trim angle at which the small boat is launched is changed between 0.0 °, 2.0 ° and 4.0 °. A positive trim angle indicates a turn that causes the bow to move upwards. In addition to the release speed of the crane cable ($v_{\mathrm{L}} = 0.4\,\frac{\mathrm{m}}{\mathrm{s}}$ $v_{\mathrm{L}} = 0.6\,\frac{\mathrm{m}}{\mathrm{s}}$ and $v_{\mathrm{L}} = 0.8\,\frac{\mathrm{m}}{\mathrm{s}}$), the forward speed is changed. The Froude numbers matching the vessels are listed in table 2. The forward speed is initially the same for both vessels and is added to the solution from the equation of motion without considering any additional propulsion force acting. This also applies to the small craft in a suspended state. For the smallest speed of $v = 3\frac{\mathrm{m}}{\mathrm{s}}$ the calculation of the stationary wave field is switched off and its influence is neglected as explained in section 2.3. During the launching process, no hydrodynamic forces act on the small craft's hull until the time of first immersion in a wave. Wind and current effects are not considered in the simulations carried out here.

4. Results of parameter study

The results for the root mean square (RMS) values for accelerations and roll angles are presented in figures 3-8. In order to assess the influence of the hydrodynamic forces on the motion during launching procedure, the simulated results are compared with limiting values for lateral and vertical acceleration and roll angle from the Nordforsk criteria [1]. These limits evaluate the general operability of the vessel under consideration. For a small fast boat, the root mean square values of 0.1 g for lateral acceleration, 0.275 g for vertical acceleration and 4.0 ° roll angle must not be exceeded. The values for the accelerations are estimated on the bridge. For this dinghy the position is assumed to be one metre vertically above the centre of gravity. For post-processing, intervals of the calculated time series are examined in which the immersion into the water occurs. The interval length is 10 s. On the x-axis of each figure, the forward speed of the

small craft is plotted as the non-dimensional Froude number. The accelerations are provided dimensionless with the gravitational acceleration.

4.1. Motion comparison

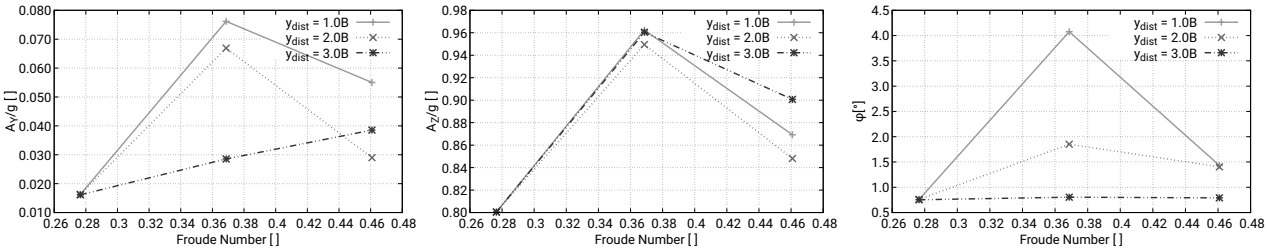

Figure 3. RMS values for lateral acceleration (left), vertical acceleration (middle) and roll angle (right) of the small craft while changing the y-distance between the two ships and $T_z = 7.5\,\mathrm{s}$.

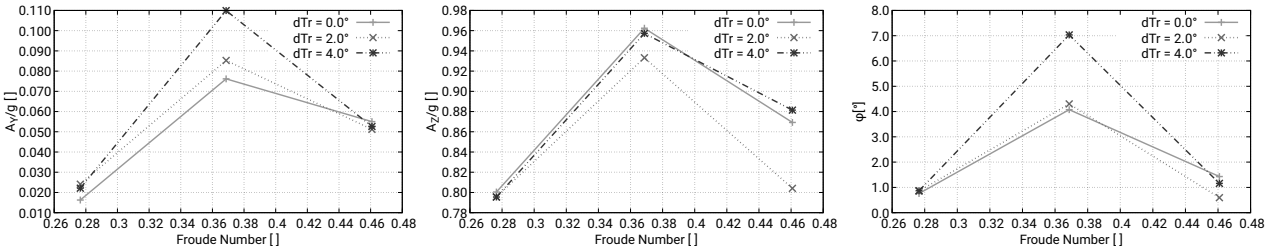

Figure 4. RMS values for lateral acceleration (left), vertical acceleration (middle) and roll angle (right) of the small craft while changing the trim angle of the small craft and d $T_z = 7.5\,\mathrm{s}$.

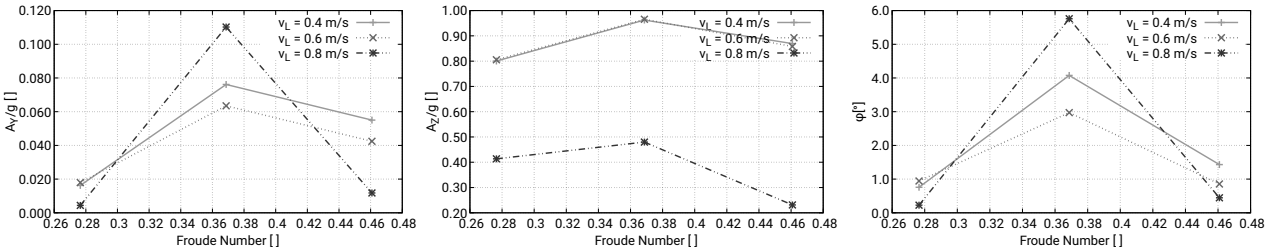

Figure 5. RMS values for lateral acceleration (left), vertical acceleration (middle) and roll angle (right) of the small craft while changing the lowering speed on the crane suspension and d $T_z = 7.5\,\mathrm{s}$.

The results are evaluated for the both sea states. First, the sea state with a smaller period $T_z = 7.5\,\mathrm{s}$ and relatively shorter waves is investigated. To be recognised is that the largest accelerations and roll angles occur with a Froude number of $Fn = 0.369$. The limits of the Nordforsk criteria for vertical accelerations are exceeded in almost all simulations. In some cases, up to 3.5 times the limit value. For the lateral accelerations, the specified limit is only exceeded in two simulations. One with a launch velocity of $v_L = 0.8\,\frac{\mathrm{m}}{\mathrm{s}}$ and one with an initial trim angle of $4.0\,^\circ$ and a Froude number of $Fn = 0.369$. The roll angle exceeds the limit especially close to the mothership (1.0 B), at the highest launch speed and the largest initial trim angle. The reason

for that is the stationary wave system is more pronounced near the mothership. Noticeable is that the launch velocity $v_{\mathrm{L}} = 0.8\,\frac{\mathrm{m}}{\mathrm{s}}$ causes significantly lower vertical accelerations, but the opposite is observed for the roll angle and lateral acceleration. The interaction between lateral acceleration and roll angle is evident. The influence of the individual parameter variations can be read off from the scattering of the values at the same forward speed. The less the scatter, the smaller the influence of this parameter on the considered variable is. The scatter is effected by Froude number especially at $Fn = 0.461$. The trim angle leads to changes in accelerations and roll angle at medium ($Fn = 0.369$) speed. The same applies to the launching speed. For one combination of parameters the Nordforsk criteria limits are not exceeded: $Fn = 0.461$, $v_{\mathrm{L}} = 0.8\,\frac{\mathrm{m}}{\mathrm{s}}$, $y_{\mathrm{dist}} = 1.0\,\mathrm{B}$ and $dTr = 0.0\,°$.

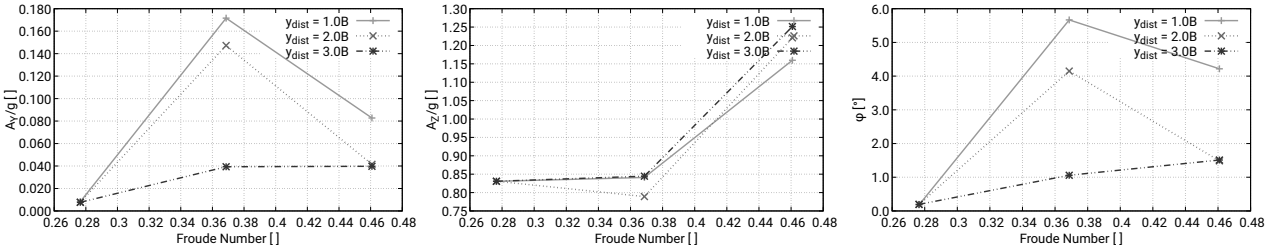

Figure 6. RMS values for lateral acceleration (left), vertical acceleration (middle) and roll angle (right) of the small craft while changing the y-distance between the two ships and $T_{\mathrm{z}} = 8.5\,\mathrm{s}$.

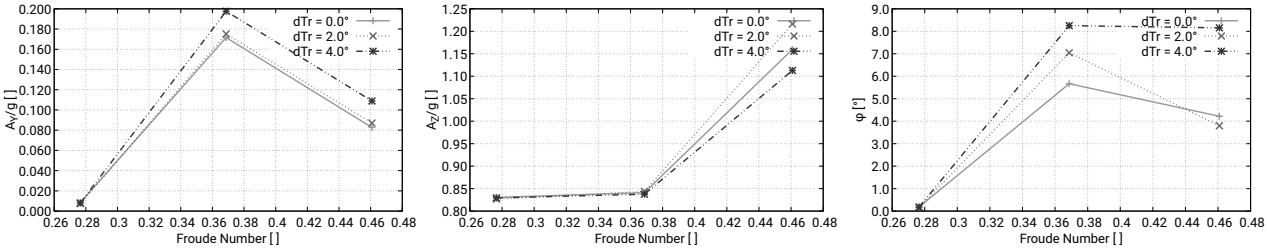

Figure 7. RMS values for lateral acceleration (left), vertical acceleration (middle) and roll angle (right) of the small craft while changing the trim angle of the small craft and $T_{\mathrm{z}} = 8.5\,\mathrm{s}$.

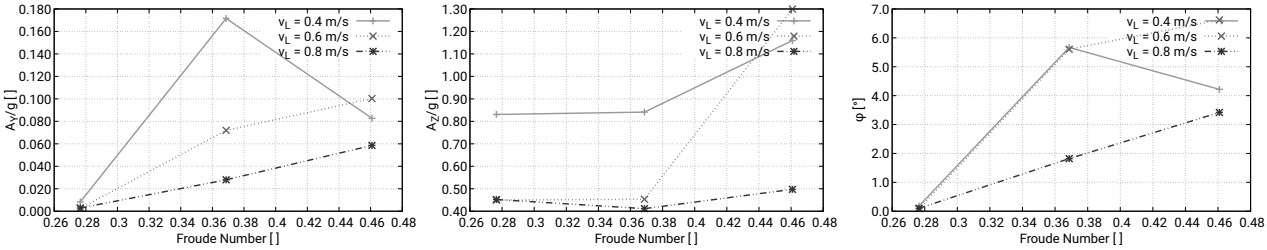

Figure 8. RMS values for lateral acceleration (left), vertical acceleration (middle) and roll angle (right) of the small craft while changing the lowering speed on the crane suspension and $T_{\mathrm{z}} = 8.5\,\mathrm{s}$.

In figures 6-8 the results for the seaway with larger wave period $T_{\mathrm{z}} = 8.5\,\mathrm{s}$ are shown. As with the other seaway, the values for vertical acceleration are greatly exceeding the threshold

of Nordforsk criteria. In this case, there is no parameter combination that leads to a values below the limit. Furthermore, the vertical accelerations for a Froude number $Fn = 0.461$ are significantly larger than for the other velocities. Limits for both the lateral accelerations and the roll angle are exceeded for the two larger forward speeds and are greater than for the seaway with a shorter period. The maximum values are twice the limit for lateral acceleration and roll angle, and up to four times higher for vertical acceleration. In comparison, an increase in lateral acceleration is particularly visible. It is noticeable that this time the highest suspension speed causes the lowest accelerations and roll angles over the entire forward speed range. The influence on the lateral acceleration and thus also the roll angle is visible especially with a Froude number $Fn = 0.369$ in combination with the launching speed and the distance between the ships. In case of vertical acceleration, only the forward speed and the launching speed have an significant influence.

4.2. Force comparison

For the force comparison, the vertical hydrodynamic radiation forces on the hull are considered. These are shown for the different parameter variations in figure 9 and 10 for $T_z = 7.5\,s$ and $T_z = 8.5\,s$, respectively. The values are plotted over the Froude numbers and depicted dimensionless by using the small craft's weight $\Delta = 5500\,kg$ and the gravitational acceleration.

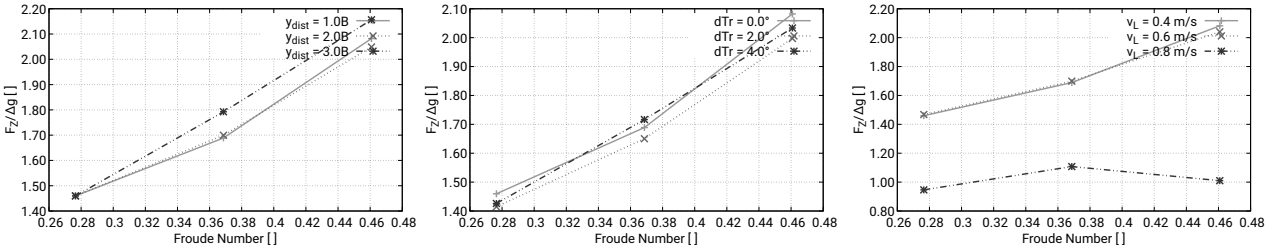

Figure 9. RMS values for the vertical force acting on the small craft for different parameter variances and $T_z = 7.5\,s$.

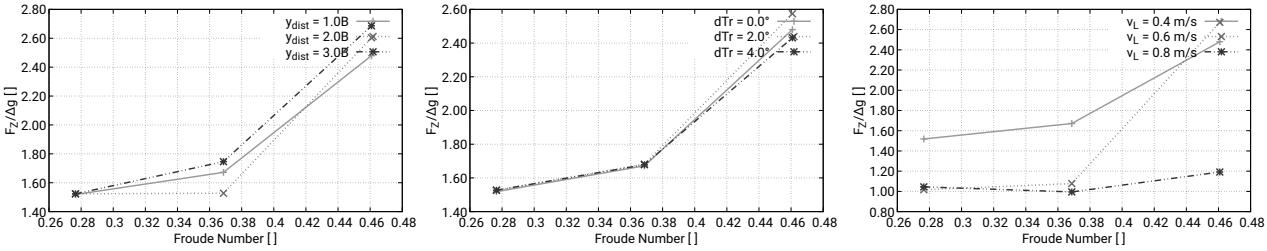

Figure 10. RMS values for the vertical force acting on the small craft for different parameter variances and $T_z = 8.5\,s$.

Apparently, the forces for both sea states and all parameter variations increase at higher forward speed. Values of $0.9 - 1.75$ times the ship weight are reached for the Froude number $Fn = 0.277$ and up to 2.7 times the ship weight for $Fn = 0.461$. The influence of changes in trim and distance between the ships is small compared to the launching speed. Notably, for a launching velocity of $v_L = 0.8\,\frac{m}{s}$, the forces are only slightly more than half as high in comparison to $v_L = 0.4\,\frac{m}{s}$.

5. Conclusion

In this paper, the influence of different parameters on the accelerations and forces during a launching procedure of a boat with a crane from a mothership was analysed. Besides the transverse distance between small craft and mothership, the initial trim angle of the dinghy, the lowering speed of the crane and different forward speeds with and without the effect of a stationary wave system are investigated. Overall, reasonable results are calculated. The launching process in combination with the selected sea state leads to exceedance of the limit values for the vertical acceleration in almost all simulations and only in some cases for the lateral acceleration and the roll angle. With regard to the accelerations and roll angles, the varied trim angle has less influence compared to the other two parameters. A low Froude number as $Fn = 0.277$ is recommended for the small craft. In terms of forces, it is a higher forward speed that leads to larger forces. In addition, the launch speed has the strongest influence. The effect of changing trim angle and the transverse distance is relatively small. By varying the parameters, a combination is obtained which leads to compliance with all limiting values of accelerations and roll angle. This is applicable for the following launch condition at a sea state with a shorter significant period: a mean transverse distance of 1.0 B, an initial trim angle of $0.0\,^{\circ}$, a high launching speed of $v_{\mathrm{L}} = 0.8\,\frac{\mathrm{m}}{\mathrm{s}}$ combined with a forward speed of $v = 5.0\,\frac{\mathrm{m}}{\mathrm{s}}$. Additional reduction of the acceleration values and roll angles can can be achieved by increasing the distance between the vessels and considering a certain initial trim angle of the small craft.

References

[1] Faltinsen O. M. 1990 *Sea Loads on Ships and Offshore Structures* (Cambridge University Press)
[2] Cummins, W. E. and United States. Navy 1962 *The Impulse Response Function and Ship Motions* (Washington DC, United States Department of the Navy, David Taylor Model Basin)
[3] Detlefsen O., Reiner C. and Abdel-Maksoud M. 2022 A Reliable Multilevel Method for Simulation-Based Load Determination in Deck Cell Guides. *Proceedings of the ASME 2022 41st International Conference on Ocean, Offshore and Arctic Engineering, OMAE. ASME, 6*
[4] El Moctar, B. O., Schellin, T. E. and Soeding, H. 2021 *Numerical Methods for Seakeeping Problems* (Springer International Publishing)
[5] Simonis H., Marleaux P. and Abdel-Maksoud M. 2021 Numerical analysis of semi-displacement vessels in head waves *33rd Symposium on Naval Hydrodynamics 2020, published jointly by the U.S. Office of Naval Research and Osaka University*
[6] Soeding H. 1993 A method for accurate force calculations in potential flow, *Ship Technology Research*, volume **40**, pages 176-186
[7] Kim W. J., Van S. H. and Kim D. H. 2001 Measurement of flows around modern commercial ship models, *Experiments in Fluids* volume **31**, pages 567578
[8] Mueller P. C. and Schiehlen, W. O. 1976 *Lineare Schwingungen* (Wiesbaden, Akademische Verlagsgesellschaft)
[9] Brown P. W. and Klosinski W. E. 1995 *Experimental Determination of the Added Inertia and Damping of Planing Boats in Roll* (Hoboken, Davidson Laboratory, Stevens Institute of Technology)
[10] DNV 2010 *Recommended Practice DNV-RP-C205 - Environmental Conditions and Environmental Loads* (Det Norske Veritas)